THE JOURNAL OF BIOLOGICAL CHEMISTRY VOL. 280, NO. 44, pp. 37195–37203, November 4, 2005

Inhibitory Interaction of the 14-3-3ϵ Protein with Isoform 4 of the Plasma Membrane Ca^{2+}-ATPase Pump*

Received for publication, May 4, 2005, and in revised form, August 25, 2005 Published, JBC Papers in Press, August 26, 2005, DOI 10.1074/jbc.M504921200

Alessandro Rimessi[‡1], **Luisa Coletto**[§¶1], **Paolo Pinton**[‡], **Rosario Rizzuto**[‡2], **Marisa Brini**[§¶], **and Ernesto Carafoli**[§¶3]

From the [§]*Department of Biochemistry, University of Padova, Viale G. Colombo 3, 35121 Padova, Italy, the* [¶]*Venetian Institute of Molecular Medicine, Via G. Orus 2, 35129 Padova, Italy, and the* [‡]*Department of Experimental and Diagnostic Medicine, Interdisciplinary Center for the Study of Inflammation, University of Ferrara, Via Borsari 46, 44100 Ferrara, Italy*

The isoform-specific interaction of plasma membrane Ca^{2+}-ATPase (PMCA) pumps with partner proteins has been explored using a yeast two-hybrid technique. The 90 N-terminal residues of two pump isoforms (PMCA2 and PMCA4), which have a low degree of sequence homology, have been used as baits. Screening of 5×10^6 clones of a human brain cDNA library yielded ~100 *LEU2*- and galactoside-positive clones for both pumps. A clone obtained with the PMCA4 bait specified the ϵ-isoform of the 14-3-3 protein, whereas no 14-3-3ϵ clone was obtained with the PMCA2 bait. The 14-3-3ϵ protein immunoprecipitated with PMCA4 (not with PMCA2) when expressed in HeLa cells. Overexpression of 14-3-3ϵ in HeLa cells together with targeted aequorins showed that the ability of the cells to export Ca^{2+} was impaired; stimulation with histamine, an inositol 1,4,5-trisphosphate-producing agonist, generated higher cytosolic $[Ca^{2+}]$ transients, higher post-transient plateaus of the cytosolic $[Ca^{2+}]$, and higher Ca^{2+} levels in the endoplasmic reticulum lumen and in the subplasmalemmal domain. Thus, the interaction with 14-3-3ϵ inhibited PMCA4. Silencing of the 14-3-3ϵ gene by RNA interference significantly reduced the expression of 14-3-3ϵ, substantially decreasing the height of the histamine-induced cytosolic $[Ca^{2+}]$ transient and of the post-transient cytosolic $[Ca^{2+}]$ plateau.

One unsolved problem in the area of plasma membrane Ca^{2+}-ATPase (PMCA)[4] pumps is the rationale for the existence of the large number of isoforms. In addition to the four basic gene products (PMCA1–4), a complex array of alternative splicing of the primary transcripts of each gene product generates a vast family of additional variants. The finding that the isoforms are differentially distributed among cells whose Ca^{2+} homeostasis needs differ substantially, *e.g.* neurons, suggests functional differences among the pump variants. These differences are unlikely to be dramatic and probably concern only subtler aspects related to regulation or even to the differential targeting to selected plasma membrane domains. The information in the literature on functional differences among pump variants is very scarce. Older findings on purified pumps or on pumps in isolated membrane preparations showed that one variant of the pump that is essentially restricted to neurons (PMCA2) has higher calmodulin affinity than the ubiquitous isoform PMCA4 (1). It has also been shown that one variant truncated C-terminally by a splicing process that changes the C-terminal part of the calmodulin-binding domain (PMCA2a or CII) has significantly reduced calmodulin affinity (2). It has also been shown that purified PMCA1 preparations are peculiarly sensitive to calpain proteolysis (3). However, the information obtained on pumps removed from the native cellular environment is necessarily incomplete, as it does not consider the possible effects of the endogenous regulators as well as the concentration of activators, *e.g.* calmodulin, available to the PMCA pumps *in vivo*. Thus, a recent study of the activity of pump variants *in vivo* has unexpectedly shown that C-terminally truncated recombinant pumps, which have reduced calmodulin affinity when tested in the isolated state, are as effective in ejecting Ca^{2+} from model cells as their full-length counterparts (4). Evidently, in the native cellular environment, sufficient calmodulin may be available to the PMCA pumps to ensure optimal Ca^{2+} extrusion even by variants that have much reduced affinity for calmodulin. The *in vivo* work has also shown that, irrespective of calmodulin, the overall Ca^{2+}-extruding ability of the two ubiquitously expressed gene products (PMCA1 and PMCA4) is much lower than that of the two tissue-specific gene products (PMCA2 and PMCA3).

An interesting contribution on splice variants, although not immediately related to function, has offered a clue to the reason for the alternative splicing at site A in the first intracellular loop. It is essential for the targeting of pump 2 to the apical region of the plasma membrane of Madin-Darby canine kidney epithelial cells (5).

The matter of endogenous regulators of the activity of PMCA pumps is now beginning to attract attention. A number of studies on possible protein partners of the pumps have appeared, and recent contributions have extended the information to their effects on pump activity. In general, these studies have not considered the possibility of isoform-specific effects, but one interesting contribution has shown that PMCA2 interacts with Na^+/H^+ exchanger regulatory factor-2, whereas PMCA4 does not (6).

Most studies searching for PMCA pump interactors have focused on the C-terminal domain of the pump, showing its ability to bind to the PDZ (PSD-95/Dlg/ZO-1) domains of partner proteins. This work has led to the identification of partners like the membrane-associated gua-

* This work was supported by Telethon Foundation of Italy Grants GGP04169 (to M. B.) and 1285 (to R. R.); the Italian Association for Cancer Research, the Italian Space Agency, and the Programma Regionale per la Ricerca Industriale, l'Innovazione, e il Trasferimento Tecnologico (to R. R.); the Human Frontier Science Program Organization (to E. C. and R. R.); the Italian Ministry of University and Scientific Research (PRIN and FIRB to M. B., E. C., and R. R.); and the National Research Council of Italy Target Project on Biotechnology and Agency 2000. The costs of publication of this article were defrayed in part by the payment of page charges. This article must therefore be hereby marked "*advertisement*" in accordance with 18 U.S.C. Section 1734 solely to indicate this fact.

[1] Both authors contributed equally to this work.

[2] To whom correspondence may be addressed. Tel.: 39-532-291-361; Fax: 39-532-247-278; E-mail: rzr@unife.it.

[3] To whom correspondence may be addressed: Dept of Biochemistry, University of Padova, Viale G. Colombo 3, 35121 Padova, Italy. Tel.: 39-49-792-3240; Fax: 39-49-792-3275; E-mail: ernesto.carafoli@unipd.it.

[4] The abbreviations used are: PMCA, plasma membrane Ca^{2+}-ATPase; cytAEQ, cytosol-targeted wild-type aequorin; h, human; GST, glutathione *S*-transferase; PBS, phosphate-buffered saline; BisTris, 2-[bis(2-hydroxyethyl)amino]-2-(hydroxymethyl)propane-1,3-diol; MOPS, 4-morpholinepropanesulfonic acid; TRITC, tetramethylrhodamine isothiocyanate; ER, endoplasmic reticulum; pmAEQmut, subplasmalemma-targeted aequorin mutant; erAEQmut, endoplasmic reticulum-targeted aequorin mutant; mtAEQmut, mitochondrion-targeted aequorin mutant; KRB, Krebs-Ringer buffer; Fura-2/AM, Fura-2 acetoxymethyl ester; $[Ca^{2+}]_c$, cytosolic free Ca^{2+} concentration; SERCA, sarcoplasmic/endoplasmic reticulum Ca^{2+}-ATPase; tBuBHQ, 2,5-di-(*tert*-butyl)-1,4-benzohydroquinone; $[Ca^{2+}]_{pm}$, subplasmalemmal $[Ca^{2+}]$.

nylate kinases (7, 8), the calcium/calmodulin-dependent serine protein kinase (9), and the neuronal NO synthetase (10). In this study, we have extended the search for interactors to the pump isoforms using a yeast two-hybrid screening procedure and the N-terminal domain (which differs most significantly among the four basic isoforms) of the pump as bait. Two isoforms were chosen for this study, one ubiquitously expressed (PMCA4) and one tissue-restricted (PMCA2). We have identified one protein partner (the 14-3-3ε protein) for PMCA4 and have found that it does not interact with PMCA2. The interaction inhibits the activity of the PMCA4 pump.

EXPERIMENTAL PROCEDURES

Cell Culture and Transfection—HeLa cells were cultured in Dulbecco's modified Eagle's medium supplemented with 10% fetal calf serum in 75-cm^2 Falcon flasks. For the aequorin experiments, the cells were seeded onto 13-mm glass coverslips and allowed to grow to 75% confluence. At this stage, transfection with 4 μg of total DNA (3 μg of the indicated expression plasmids + 1 μg of aequorin) was carried out as described previously (11). For co-immunoprecipitation experiments, HeLa cells were grown on 6-well plates and transfected with the expression plasmid for PMCA4 (pSG5/PMCA4) or for PMCA2 (pcDNA3/PMCA2) at 6 μg/well. For small interfering RNA experiments, HeLa cells were plated onto 10-cm Petri dishes and transfected with 16 μg of DNA (14 μg of mitochondrion-targeted green fluorescent protein + 2 μg of cytosol-targeted wild-type aequorin (cytAEQ) in control cells or 14 μg of pSUPER/14-3-3ε + 2 μg of cytAEQ). Aequorin measurements or co-immunoprecipitation experiments were performed 36 h after transfection. The expression plasmid for 14-3-3ε (pEGFP-C1/14-3-3ε) was kindly provided by Dr. S. Volinia (University of Ferrara).

Plasmid Constructions—The region encoding the N-terminal portion (residues 2–92) of human (h) PMCA4 and PMCA2 was amplified by 30 cycles of PCR (denaturation at 95 °C for 1 min, annealing at 60 °C for 45 s, and extension at 72 °C for 1 min) using the following oligonucleotides (with the restriction sites underlined): hPMCA2, 5′-CCGGAATTCGGTGACATGAC-3′ (sense) and 5′-CGCGGATCCGCTTTCTTTGGAG-3′ (antisense); and hPMCA4, 5′-CCGGAATTCACGAACCCATC-3′ (sense) and 5′-CGCGGATCCAAGTCTTGGGC-3′ (antisense). The amplified products were digested with EcoRI and BamHI and cloned in-frame into the cloning sites of plasmid pGilda (Clontech) to generate the DNA-binding fusions (pGilda-P2 and pGilda-P4) for yeast two-hybrid screening and assays. The same sequences were cloned with the appropriate restriction enzymes into the pGEX-4TK vector (Amersham Biosciences) to produce glutathione *S*-transferase (GST) fusion proteins (GST-P2 and GST-P4).

The mammalian expression vector pSUPER (Oligoengene) was used for the expression of small interfering RNA in HeLa cells. The gene-specific insert specifies a 19-nucleotide sequence corresponding to nucleotides 539–557 downstream of the transcription start site (ggaggctgcggagaacagc) of 14-3-3ε, which is separated by a 9-nucleotide noncomplementary spacer (ttcaagaga) from the reverse complement of the same 19-nucleotide sequence. This sequence was inserted into the pSUPER vector backbone after digestion with BglII and HindIII. This vector is referred to as pSUPER/14-3-3ε and was transformed into DH5α competent cells according to the manufacturer's instructions (Oligoengene). After plating on LB medium supplemented with ampicillin, colonies were selected, and the vector was amplified. Positive colonies were identified by the presence of an EcoRI-HindIII restriction fragment of ~290 bp. (The corresponding fragment from the empty vector is 227 bp.)

Yeast Two-hybrid Library Screening—Yeast two-hybrid screening was carried out according to the standard protocol recommended by Clontech. The bait plasmid pGilda and the p8op-*lacZ* reporter gene plasmid were first transformed in yeast EGY48 cells, followed by transformation of the library of brain cDNA plasmids. Approximately 5 × 10^6 yeast cells cotransformed with the bait, and cDNAs from a premade human brain cDNA Matchmaker LexA library (Invitrogen) were screened. Positive clones were selected for their ability to grow on plates lacking leucine, tryptophan, histidine, and uracil and were assayed for β-galactosidase activity on medium supplemented with 5-bromo-4-chloro-3-indolyl-β-D-galactopyranoside (X-gal). Plasmids containing the brain cDNAs were isolated from positive yeast cells, and their nucleotide sequences were determined by DNA sequencing. The plasmid containing the positive cDNA was isolated from yeast by a miniprep protocol. The cells of the positive clone were resuspended in 1 M sorbitol and 50 mM EDTA with the yeast lytic enzyme (2 mg/ml; MP Biomedicals). After 30 min at 37 °C, the yeast cells were centrifuged, and the pellet was dissolved in Hirt's solution (10 mM Tris-Cl (pH 7.5), 50 mM EDTA, and 0.2% SDS) with 0.5 mg/ml proteinase K (Invitrogen) and incubated at 50 °C for >6 h. The plasmid DNA was extracted with phenol/chloroform/isoamyl alcohol (25:24:1). The aqueous phase was precipitated with the same volume of 20% polyethylene glycol and 2.5 M NaCl, and the plasmid DNA was pelleted, washed with 70% ethanol, and resuspended in 10 μl of 10 mM Tris-HCl (pH 7.5) and 1 mM EDTA. The plasmid obtained was transformed into *Escherichia coli* strain DH5α by electroporation.

Co-immunoprecipitations—After 36 h, HeLa cells were rinsed with cold Ca^{2+}- and Mg^{2+}-free phosphate-buffered saline (PBS) and lysed in buffer A (50 mM HEPES (pH 7.4), 150 mM NaCl, 1% Nonidet P-40, 0.5% sodium deoxycholate, and protease inhibitor mixture (Roche Applied Science)). After 30 min on ice, the cells were scraped from the plates using a rubber policeman and centrifuged at 11,000 × *g* for 10 min at 4 °C. 500 μg were used for each immunoprecipitation, to which 2–3 μl of antibody (anti-PMCA monoclonal antibody 5F10, Affinity BioReagents, Golden, CO) were added. After 3 h of rocking at 4 °C, 50 μl of protein A/G-agarose (Santa Cruz Biotechnology, Inc.) were added to each mixture, and rocking was continued overnight at 4 °C. Protein A/G-agarose was pelleted at 4000 × *g* for 30 s. The immune complex beads were quickly washed three times with cold PBS. All of the bound protein and 5% of the starting lysate (input) were separated on 10% NuPAGE BisTris gel with MOPS running buffer (Invitrogen); transferred to polyvinylidene difluoride membrane; and incubated with rabbit anti-14-3-3ε, anti-14-3-3ζ, and anti-14-3-3θ polyclonal antibodies (Santa Cruz Biotechnology, Inc.).

GST Fusion Protein Expression and Pull-down Assay—GST and GST-P2 and GST-P4 fusion proteins were expressed in *E. coli* BL21 by incubation in LB medium supplemented with 1 mM isopropyl 1-thio-β-D-galactopyranoside and ampicillin at 37 °C for 2 h. Cells were pelleted and sonicated in Tris-buffered saline (50 mM Tris-HCl (pH 8.0) and 150 mM NaCl) plus protease inhibitors. GST fusion proteins were purified by incubation with glutathione-Sepharose beads (Amersham Biosciences) at 4 °C for 1 h. After washing three times with Tris-buffered saline, the concentrations and integrity of the fusion proteins were estimated by SDS-PAGE and subsequent Coomassie Blue staining. For pull-down assay, the HeLa cells were lysed in buffer A. Equal amounts of total lysate of cells expressing equivalent levels of endogenous 14-3-3 isoforms (ε, ζ, and θ) were incubated with Sepharose beads containing GST, GST-P2, or GST-P4 and rocked at 4 °C for 2 h. After three washings with Tris-buffered saline, the bound proteins were eluted with Laemmli loading buffer; separated on 10% NuPAGE BisTris gel with

MOPS running buffer; transferred to polyvinylidene difluoride membrane; and incubated with rabbit anti-14-3-3ε, anti-14-3-3ζ, and anti-14-3-3θ polyclonal antibodies and mouse anti-GST monoclonal antibody (Santa Cruz Biotechnology, Inc.).

Immunofluorescence Experiments—HeLa cells were plated onto 24 × 24-mm coverslips at a density of 3×10^5 cells/coverslip. Transfected cells (hPMCA4 and 14-3-3ε) were washed with PBS, warmed at 37 °C, and fixed with 4% paraformaldehyde for 20 min at room temperature. Cells were washed twice with PBS and permeabilized with 0.2% Triton X-100 in PBS for 5 min. Unspecific staining was reduced by blocking with 10% horse serum for 30 min. Cells were incubated overnight with a 0.1% (v/v) solution of mouse anti-PMCA4 monoclonal antibody (Sigma) in 1% horse serum and a 0.1% solution of anti-14-3-3ε polyclonal antibody in 1% horse serum. Following incubation, cells were washed three times with PBS. Antibodies that bound to PMCA4 or 14-3-3ε were detected by incubating the cells for 2 h in the dark with a 1% (v/v) solution of fluorescein isothiocyanate-conjugated sheep anti-mouse IgG (Santa Cruz Biotechnology, Inc.) or TRITC-conjugated goat anti-rabbit IgG (Santa Cruz Biotechnology, Inc.) in 1% horse serum. Unbound antibody was removed by washing three times with PBS. Fluorescence was visualized using a digital imaging system based on a Zeiss Axiovert 200 fluorescence microscope equipped with a back-illuminated CCD camera (Roper Scientific) with a ×63 objective and appropriate filters. Some cells were treated only with secondary antibodies and used to calculate background values (due to unspecific binding) in the samples. The data were acquired and processed using MetaMorph Version 5.0 software (Universal Imaging Corp.). *Z*-series images were deconvolved using exhaustive photon reassignment EPR software, a point spread function-based deconvolution algorithm developed by the University of Massachusetts Imaging Group (12), running on a Linux-based personal computer.

Aequorin Measurements—The probes employed are chimeric aequorins targeted to the cytosol (cytAEQ), subplasmalemmal region (pmAEQmut), endoplasmic reticulum (ER; erAEQmut), and mitochondria (mtAEQmut). "AEQ" refers to wild-type aequorin, and "AEQmut" refers a low affinity D119A mutant of aequorin. For a map of the constructs and detailed information on their characteristics, see Ref. 13. Reconstitution protocols were different for cytAEQ and mtAEQmut and for erAEQmut and pmAEQmut. For the experiments with cytAEQ and mtAEQmut, cells were incubated with 5 μM coelenterazine for 1–2 h in Dulbecco's modified Eagle's medium supplemented with 1% fetal calf serum. A coverslip with transfected cells was placed in a perfused thermostatted chamber located in close proximity to a low noise photomultiplier with a built-in amplifier/discriminator. To reconstitute erAEQmut with high efficiency, the luminal $[Ca^{2+}]$ of the ER first had to be reduced. This was achieved by incubating the cells for 1 h at 4 °C in Krebs-Ringer buffer (KRB) supplemented with 5 μM coelenterazine, 5 μM Ca^{2+} ionophore ionomycin (Sigma), and 600 μM EGTA. After this incubation, cells were extensively washed with KRB supplemented with 2% bovine serum albumin and then transferred to the perfusion chamber. For recombinant aequorin pmAEQmut reconstitution, the cells were transferred to modified KRB (125 mM NaCl, 5 mM KCl, 1 mM Na_3PO_4, 1 mM $MgSO_4$, 5.5 mM glucose, and 20 mM HEPES (pH 7.4)) supplemented with 100 μM EGTA and 5 μM coelenterazine at 37 °C. After 45 min, the coverslip was transferred to the luminometer chamber and perfused with KRB containing 100 μM EGTA.

All aequorin measurements were carried out in KRB supplemented with either 1 mM $CaCl_2$ (cytAEQ and mtAEQmut) or 100 μM EGTA (erAEQmut and pmAEQmut). Agonist and other drugs were added to the same medium as specified in the figure legends. The experiments were terminated by lysing the cells with 100 μM digitonin in a hypotonic Ca^{2+}-containing solution (10 mM $CaCl_2$ in H_2O), thus discharging the remaining aequorin pool. The output of the discriminator was captured by a Thorn EMI photon-counting board and stored in an IBM-compatible computer for further analyses. The aequorin luminescence data were calibrated offline into $[Ca^{2+}]$ values using a computer algorithm based on the Ca^{2+} response curve of wild-type and mutant aequorins as described previously (14). Chemicals and reagents were from Sigma or Merck, except for coelenterazine and coelenterazine *n*, which were from Molecular Probes, Inc. Statistical data are presented as means ± S.E.

Fura-2 Acetoxymethyl Ester (Fura-2/AM) Measurements—The cytosolic free Ca^{2+} concentration ($[Ca^{2+}]_c$) was evaluated using the fluorescent Ca^{2+} indicator Fura-2/AM (Molecular Probes, Inc.). Briefly, cells were incubated in medium supplemented with 2.5 μM Fura-2/AM for 30 min, washed with KRB to remove the extracellular probe, supplied with preheated KRB (supplemented with 1 mM $CaCl_2$), and placed in a thermostatted (37 °C) incubation chamber on the stage of an inverted fluorescence microscope (Zeiss Axiovert 200). Dynamic video imaging was performed using MetaFluor software (Universal Imaging Corp.). Fluorescence was measured every 100 ms with the excitation wavelength alternating between 340 and 380 nm and the emission fluorescence being recorded at 510 nm. At the end of the experiment, a region free of cells was selected, and one averaged background frame was collected at each excitation wavelength for background correction. The $[Ca^{2+}]_c$ was calculated by the ratio method using the following equation: $[Ca^{2+}]_c = K_d(R - R_{min})/(R - R_{max}) \times Sf2/Sf1$, where K_d is the dissociation constant of Fura-2/AM for Ca^{2+} taken as 240 nM at 37 °C, *R* is the ratio of fluorescence for Fura-2/AM at the two excitation wavelengths (F_{340}/F_{380}), R_{min} is the ratio of fluorescence in the presence of minimal calcium obtained by lysing the cells and then chelating all the Ca^{2+} with 0.5 M EGTA, R_{max} is the ratio of fluorescence in the presence of excess calcium obtained by lysing the cells with 10 μM ionomycin, *Sf2* is the fluorescence of the Ca^{2+}-free form of Fura-2/AM at an excitation wavelength of 380 nm, and *Sf1* is the fluorescence of the Ca^{2+}-bound form of Fura-2/AM at an excitation wavelength of 380 nm.

Western Blot Analysis of Small Interfering RNA Expression—36 h after transfection, cells were washed twice with PBS, scraped, centrifuged at 1000 × *g* for 5 min, resuspended in 80 μl of buffer A, and kept on ice for 20 min. Lysates were centrifuged at 11,000 × *g* for 20 min, and then the supernatants were harvested. The proteins (5 μg) were separated on 12% polyacrylamide gel and transferred to polyvinylidene difluoride membrane. The amounts of endogenous 14-3-3ε and the marker protein β-tubulin were estimated by Western blotting using rabbit anti-14-3-3ε polyclonal antibody and mouse anti-β-tubulin antibody (Santa Cruz Biotechnology, Inc.).

RESULTS

Binding of 14-3-3ε to the PMCA Pumps—To identify proteins that interact with the N-terminal sequence of PMCA pumps, we used as bait a construct consisting of the LexA DNA-binding domain of pGilda fused to the first 90 amino acids of PMCA4 or PMCA2 to screen a human brain cDNA library. The N-terminal region was chosen because of its low degree of homology among PMCA pumps (~50% amino acid identity).

Approximately 100 *LEU2*- and galactosidase-positive clones were obtained from both pumps upon screening 5×10^6 clones. Sequencing of the cDNA inserts revealed that a clone obtained using the PMCA4 bait specified amino acids 5–55 of the 14-3-3 protein.

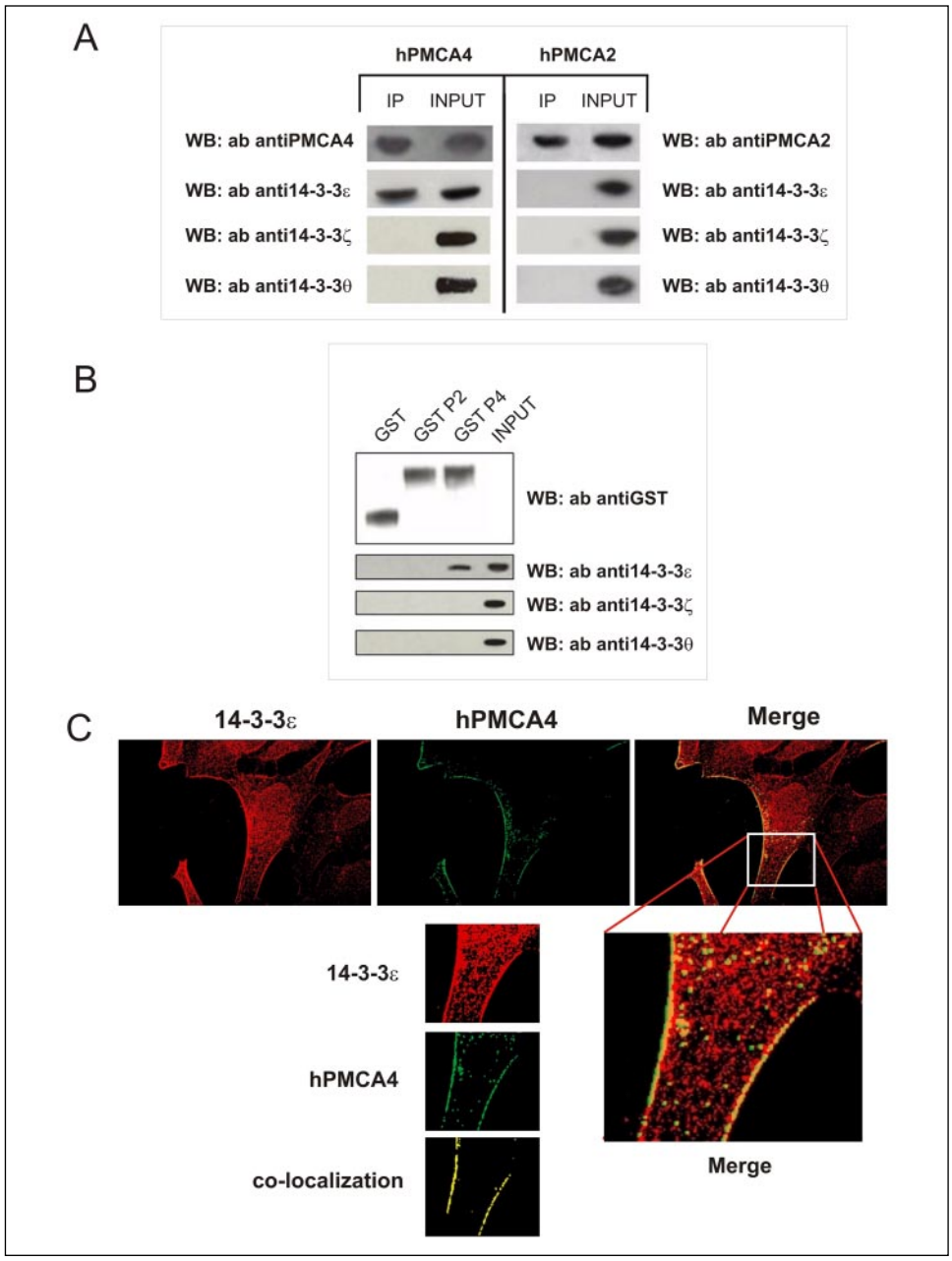

FIGURE 1. *A*, co-immunoprecipitations of 14-3-3 isoforms with PMCA4 and PMCA2. HeLa cells were transfected with the expression plasmid encoding hPMCA4 (pSG5/PMCA4) or hPMCA2 (pcDNA3/PMCA2) as indicated on the top of each panel. After 36 h, cells were lysed, and 5% of the protein lysate was used directly as input for NuPAGE Bis-Tris gel. The remaining cell lysate was immunoprecipitated (*IP*) with anti-PMCA antibody 5F10 as described under "Experimental Procedures." Western blots (*WB*) of the separated proteins were then probed with the isoform-specific PMCA antibodies (*ab*; 2N for PMCA2 and 4N for PMCA4) and with antibodies specific for the isoforms of 14-3-3 to detect the proteins as indicated. Note that the 14-3-3ϵ protein precipitated with PMCA4, but not with PMCA2, and that 14-3-3θ and 14-3-3ζ did not precipitate with either PMCA2 or PMCA4. *B*, protein pull-down experiments confirming the interaction between PMCA4 and 14-3-3ϵ. Equal aliquots of lysates from HeLa cells were incubated with Sepharose beads containing GST alone and GST fused to the N-terminal domains of PMCA2 (GST-P2) and PMCA4 (GST-P4). Bound proteins were separated on 10% NuPAGE gel and transferred to polyvinylidene difluoride membranes. The membranes were probed with antibodies against 14-3-3ϵ, 14-3-3θ, and 14-3-3ζ. 5% of the total lysates was used as input. The expression levels of the ϵ-, θ-, ζ-isoforms were comparable, as demonstrated by the input. 14-3-3ϵ bound to PMCA4, but not to PMCA2. None of the 14-3-3 isoforms bound to GST alone. *C*, 14-3-3ϵ and PMCA4 co-localize in HeLa cells. Double immunofluorescence staining of hPMCA4 and 14-3-3ϵ showed co-localization in HeLa cells. The cells were cotransfected with the expression vectors for 14-3-3ϵ and hPMCA4. The localization of the PMCA4 and 14-3-3ϵ proteins was detected by incubation with anti-PMCA4 monoclonal antibody (*middle panel*) and rabbit anti-14-3-3ϵ polyclonal antibody (*left panel*), respectively. Bound anti-14-3-3ϵ antibodies were stained by secondary incubation with TRITC-conjugated goat anti-rabbit IgG (*red*), whereas anti-PMCA4 antibodies were stained by secondary incubation with fluorescein isothiocyanate-conjugated sheep anti-mouse IgG (*green*). The merged image (*right panel*) shows the co-localization of hPMCA4 and 14-3-3ϵ at the plasma membrane. The larger magnification of the images in the *insets* allows a better appreciation of the protein distribution. The *co-localization inset* shows the merged image cleaned of non-overlapping 14-3-3ϵ and hPMCA4 signals.

This clone was sequenced and identified as the ϵ-isoform of the 14-3-3 protein. To confirm that an interaction had indeed occurred, the yeast EGY48 positive clone was isolated, and the plasmid containing the cDNA corresponding to amino acids 5–55 of the identified 14-3-3ϵ partner was extracted. The purified plasmid was cotransformed with the plasmid bait (pGilda-P4) and used in the β-galactosidase assay. The results confirmed the interaction between the two proteins. No clones specifying the 14-3-3 protein were obtained with the PMCA2 bait.

Selective Co-immunoprecipitation and Co-localization of PMCA4 with the 14-3-3ϵ Protein—Based on the high degree of homology (~65% identity) of the first 55 residues of different 14-3-3 isoforms, we decided to analyze the interaction between PMCA pumps and the ϵ-, θ-, and ζ-isoforms of 14-3-3. (The θ- and ζ-isoforms have 65 and 68% homology to the ϵ-isoform, respectively.) All three isoforms are abundantly expressed in HeLa cells. To test the ability of PMCA4 and PMCA2 to bind the different isoforms of the 14-3-3 protein in the cellular environment, we transiently transfected HeLa cells with the pcDNA3/PMCA2 or pSG5/PMCA4 plasmid construct. 14-3-3ϵ was co-immunoprecipitated by anti-PMCA antibody 5F10 with PMCA4, but not with PMCA2 (Fig. 1*A*). 14-3-3θ and 14-3-3ζ failed to immunoprecipitate with either PMCA4 or PMCA2. Pull-down assays with HeLa lysates using the GST fusion proteins of the N-terminal domains of PMCA4 (GST-P4) and PMCA2 (GST-P2) confirmed that the interaction with PMCA4 was specific for 14-3-3ϵ (Fig. 1*B*). To further substantiate the physical interaction between PMCA4 and 14-3-3ϵ in HeLa cells, we cotransfected them with the PMCA4 and 14-3-3ϵ expression plasmids and analyzed the localization of the recombinant proteins by immunofluorescence. PMCA4 and 14-3-3ϵ were detected by staining with a monoclonal antibody that specifically recognizes PMCA4 and with anti-14-3-3ϵ antibody, respectively. PMCA4 localized at the plasma membrane of transfected cells (Fig. 1*C*). 14-3-3ϵ localized at the plasma membrane and in the cytosol (Fig. 1*C*). The merged image shows co-localization of PMCA4 and 14-3-3ϵ (Fig. 1*C*). Samples incubated with only second-

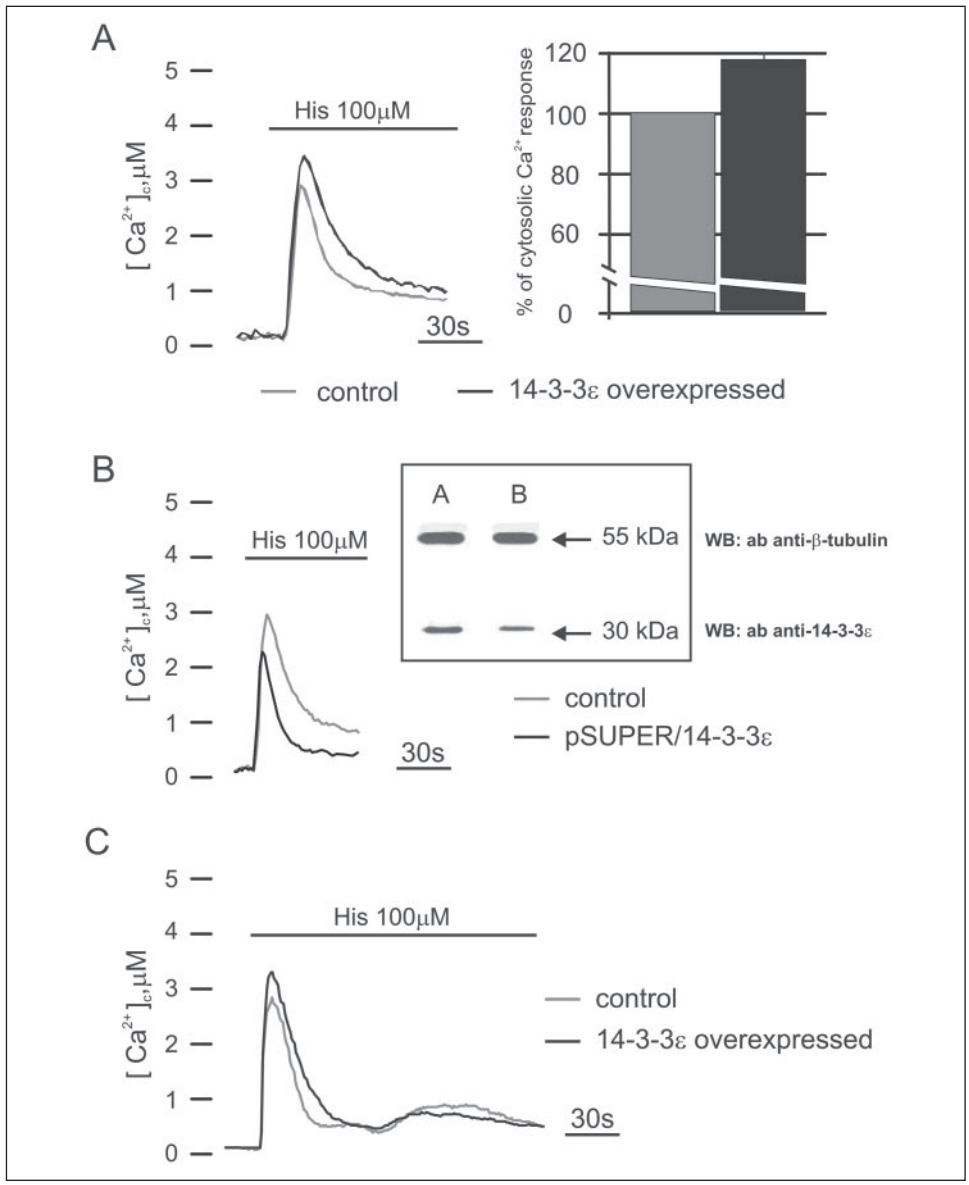

FIGURE 2. *A*, effect of 14-3-3ϵ overexpression on cytosolic Ca^{2+} homeostasis in HeLa cells. $[Ca^{2+}]_c$ measurements were performed in HeLa cells transfected with cytAEQ (*control*, *gray trace*) or cotransfected with cytAEQ and 14-3-3ϵ (*14-3-3ϵ overexpressed*, *black trace*). Where indicated, HeLa cells were challenged with 100 μM histamine (*His*). The *bars* in the graph show the extent of the increase in the $[Ca^{2+}]_c$ peak induced by overexpressing 14-3-3ϵ after cell stimulation, expressed as a percent of the response in control cells. *B*, reduced expression of 14-3-3ϵ has an effect on calcium homeostasis. $[Ca^{2+}]_c$ in control and pSUPER/14-3-3ϵ-transfected HeLa cells was monitored with cytAEQ. Where indicated, cells were stimulated with 100 μM histamine. *Inset*, overexpression of pSUPER/14-3-3ϵ resulted in significant reduction of 14-3-3ϵ expression (~35%). *C*, measurement of $[Ca^{2+}]_c$ in control and 14-3-3ϵ-transfected cells. $[Ca^{2+}]_c$ was measured using Fura-2 on an inverted fluorescence microscope (Zeiss Axiovert 200) as described under "Experimental Procedures." Histamine-evoked $[Ca^{2+}]_c$ changes in 14-3-3ϵ-expressing (*black trace*) and control (*gray trace*) cells are shown. Cells were stimulated with 100 μM histamine where indicated. The traces are representative of >10 trials.

ary antibodies, fluorescein isothiocyanate-conjugated anti-mouse IgG or TRITC-conjugated anti-rabbit IgG, did not show any staining (data not shown), confirming the specificity of the immunofluorescence detection. These results thus substantiate the finding of an interaction between PMCA4 and 14-3-3ϵ.

Effects of 14-3-3ϵ Overexpression on Calcium Signaling in HeLa Cells—The above results prompted us to investigate whether the interaction with 14-3-3ϵ has any effect on the activity of PMCA4, *i.e.* whether the overexpression of 14-3-3ϵ affects intracellular calcium homeostasis. Recombinant aequorins were cotransfected with 14-3-3ϵ in HeLa cells, which express endogenous PMCA4 (15). Because the two recombinant proteins were expressed by the same subset of cells, the risks associated with the use of stable clones or single cells were eliminated. As analyzed in detail in our previous studies (14), this approach was preferred to the isolation and analysis of stable clones coexpressing the photoprotein and the protein under investigation. The latter approach would be unavoidably plagued by the high intrinsic variability of clones, which, in most case, would mask the effects of the protein of interest. Conversely, transient coexpression of the probe and the protein of interest allows the monitoring of a proportion of the transfected cell population (~30–40%) and thus better represents the behavior of the parental population. Under these conditions, the effects observed can be reliably ascribed to the transfected population (for more details, see Ref. 14).

Fig. 2*A* shows $[Ca^{2+}]_c$ monitored with cytAEQ in control cells and in HeLa cells cotransfected with cytAEQ and 14-3-3ϵ. 36 h after transfection, cells were challenged with histamine (100 μM) in medium containing 1 mM $CaCl_2$. The stimulation caused a rapid rise in $[Ca^{2+}]_c$ in both sets of transfected cells, which was followed by a gradual decline of the trace to a lower plateau. However, the $[Ca^{2+}]_c$ increase evoked by histamine in 14-3-3ϵ-transfected cells was significantly higher than in control cells (~18%) and was followed by a slower declining phase (peak amplitude of 3.38 ± 0.07 μM ($n = 11$) *versus* 2.95 ± 0.12 μM ($n = 15$); $p < 0.01$). The data suggest an inhibitory effect of 14-3-3ϵ on the function of PMCA, resulting in an increased height and a reduced clearance rate of the $[Ca^{2+}]$ transient. To confirm this effect, we calculated, from the slope of the declining phase of the $[Ca^{2+}]$ transient, the velocity of the Ca^{2+}-extruding activity at 2 μM Ca^{2+} and found it to be ~20% higher (0.171 ± 0.02 μM/s ($n = 15$) in control cells and 0.132 ± 0.010 μM/s ($n = 11$) in 14-3-3ϵ-overexpressing cells; $p < 0.01$).

To reinforce the suggestion that 14-3-3ε acts as an inhibitor of the Ca^{2+}-extruding activity of PMCA4, we decided to investigate whether the reduced expression of 14-3-3ε has any effect on calcium homeostasis in HeLa cells. The 14-3-3ε gene was silenced using a pSUPER vector. Fig. 2*B* (*inset*) shows that transfection with a pSUPER vector expressing oligonucleotides directed against 14-3-3ε induced a significant reduction of its expression. Cells transfected with the vector had a greater ability to extrude Ca^{2+} when challenged with histamine (Fig. 2*B*). The peak of the $[Ca^{2+}]$ transient was lower, and the rate of extrusion (as deduced from the rate of $[Ca^{2+}]_c$ decline) was higher in cells with lower amounts of 14-3-3ε (2.95 ± 0.12 μM ($n = 15$) in control cells *versus* 2.31 ± 0.21 μM ($n = 15$) in 14-3-3ε-silenced cells; $p < 0.01$). This strongly indicates 14-3-3ε-linked inhibition of PMCA activity. Finally, we directly calculated the extrusion rate at a fixed $[Ca^{2+}]_c$ of 2 μM; in 14-3-3ε-silenced cells, this was ~30% higher (0.140 ± 0.011 μM/s ($n = 15$) in control cells *versus* 0.191 ± 0.011 μM/s ($n = 15$) in 14-3-3ε-silenced cells; $p < 0.01$).

To confirm the role of 14-3-3ε as a modulator of cytosolic calcium homeostasis and as an inhibitor of the Ca^{2+}-extruding activity of PMCA4, we then investigated $[Ca^{2+}]_c$ using the fluorescent Ca^{2+} indicator Fura-2/AM in HeLa cells. Cells were incubated in medium supplemented with 2.5 μM Fura-2/AM for 30 min, and fluorescence was measured and calibrated as described under "Experimental Procedures." In good agreement with the aequorin data, stimulation with histamine induced higher $[Ca^{2+}]_c$ peaks in 14-3-3ε-expressing cells than in control cells (2.89 ± 0.93 μM ($n = 12$) in control cells *versus* 3.24 ± 0.86 μM ($n = 12$) in 14-3-3ε-expressing cells; $p < 0.01$) (Fig. 2*C*).

The results thus substantiate the suggestion that the 14-3-3ε protein inhibits PMCA4 activity. A possible explanation for the increased agonist-dependent $[Ca^{2+}]_c$ response in cells transfected with 14-3-3ε is the increased amount of Ca^{2+} released by the agonist-sensitive Ca^{2+} stores (the ER) as a consequence of a higher level of Ca^{2+} filling the ER lumen. This was tested by directly monitoring the intraluminal $[Ca^{2+}]$ with erAEQmut. HeLa cells were cotransfected with erAEQmut and 14-3-3ε, and the intraluminal $[Ca^{2+}]$ values were compared. Under the experimental conditions, the intraluminal $[Ca^{2+}]$ was <10 μM in Ca^{2+}-depleted cells, and it gradually increased upon switching the perfusion medium to buffer supplemented with 1 mM Ca^{2+}, reaching a plateau level in control cells of ~250 μM. In 14-3-3ε-expressing cells, $[Ca^{2+}]$ in the ER lumen reached a 28% higher steady-state level (~320 μM) (Fig. 3*A*). At least in principle, a higher steady state of intraluminal $[Ca^{2+}]$ should increase the mitochondrial Ca^{2+} uptake after histamine stimulation. This was indeed found to be the case, as HeLa cells cotransfected with mtAEQmut and 14-3-3ε showed a peak of mitochondrial response that was markedly increased (almost 25%) with respect to control cells when challenged with histamine (data not shown).

14-3-3ε and Sarcoplasmic/Endoplasmic Reticulum Ca^{2+}-ATPase (SERCA) Pump Activity—Although the results presented here are consistent with the hypothesis that the 14-3-3ε protein inhibits PMCA activity, a positive effect of 14-3-3ε on the activity of the SERCA pump could also be considered. However, two different sets of observations militate against the involvement of the SERCA pump. The first is the response of the erAEQmut measurements (Fig. 3*A*). During the first phase of ER Ca^{2+} refilling, *i.e.* when the SERCA activity would be expected to be higher, the uptake rate was the same in control and 14-3-3ε-overexpressing cells.

The second observation is the result of a series of experiments in which the kinetics of the cytosolic calcium response evoked by perfusing cells with the SERCA pump inhibitor 2,5-di-(*tert*-butyl)-1,4-benzohydroquinone (tBuBHQ) was analyzed in 14-3-3ε-transfected and control HeLa cells (Fig. 3*B*). The inhibitor promoted only a small transient increase in $[Ca^{2+}]_c$ due to release of Ca^{2+} from the ER. If the 14-3-3ε protein had exclusively inhibited SERCA pump activity, any effect would have disappeared after tBuBHQ application. In contrast, if the target of the 14-3-3ε protein had been the PMCA pump, a more sustained $[Ca^{2+}]_c$ increase should have been observed in cells overexpressing 14-3-3ε. Fig. 3*B* shows that this was indeed the case; the amplitude of the responses was the same in control and 14-3-3ε-transfected cells

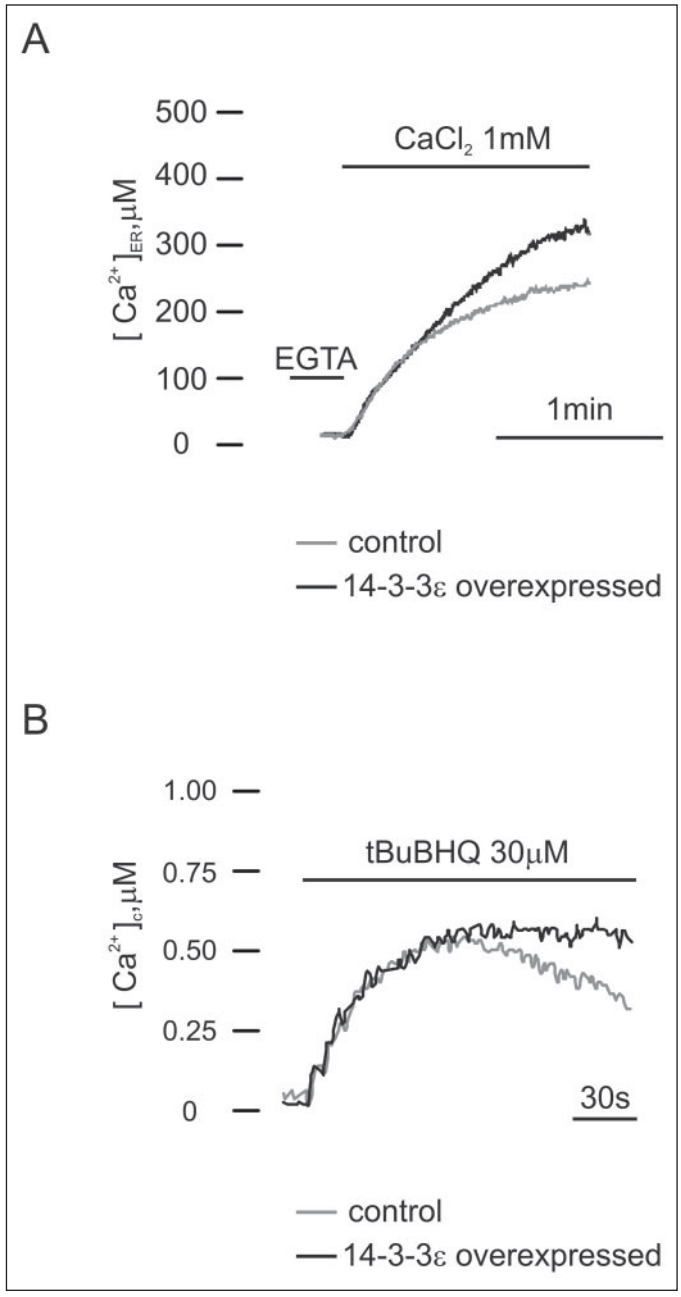

FIGURE 3. **Effect of Ca^{2+} re-addition to cells maintained in Ca^{2+}-free medium transfected with erAEQmut.** *A*, Ca^{2+} homeostasis in the lumen of the ER in control and 14-3-3ε-overexpressing HeLa cells. The cells were either cotransfected with erAEQmut and 14-3-3ε or transfected with erAEQmut alone. 36 h after transfection, the Ca^{2+} stores were depleted of Ca^{2+} to optimize aequorin reconstitution as described under "Experimental Procedures." After reconstitution, the cells were transferred to the luminometer chamber, and the ER store was refilled by switching the perfusion medium from KRB/EGTA to KRB containing 1 mM $CaCl_2$. $[Ca^{2+}]_{ER}$, intraluminal $[Ca^{2+}]$. *B*, kinetics of the cytosolic calcium response evoked by perfusing tBuBHQ (30 μM) in control and 14-3-3ε-transfected cells. $[Ca^{2+}]_c$ was measured with cytAEQ. The perfusion of the SERCA blocker tBuBHQ evoked a small transient increase in $[Ca^{2+}]_c$ due to the release of Ca^{2+} from the ER store. Although the amplitude of the $[Ca^{2+}]_c$ rise was the same in 14-3-3ε-overexpressing and control cells, the return toward basal values was markedly faster in control cells.

treated with tBuBHQ, but a markedly slower Ca^{2+} extrusion rate was observed in cells overexpressing 14-3-3ε.

Effect of 14-3-3ε on the Subplasmalemmal Ca^{2+} Level—In another set of experiments, pmAEQmut fused with SNAP-25 (soluble *N*-ethylmaleimide-sensitive factor attachment protein-25), a protein that is recruited to the plasma membrane after the post-translational addition of a lipid anchor, was used to analyze the calcium concentration in the subplasmalemmal region ($[Ca^{2+}]_{pm}$). In all experiments, $[Ca^{2+}]_{pm}$ was monitored in cells transiently expressing pmAEQmut after a 45-min reconstitution with coelenterazine in Ca^{2+}-free KRB. A major increase in $[Ca^{2+}]_{pm}$ due to Ca^{2+} influx through plasma membrane channels was observed when the perfusing buffer was supplemented with 1 mM $CaCl_2$. Fig. 4*A* (*inset*) shows that there were no significant differences in $[Ca^{2+}]_{pm}$ between batches of HeLa cells transfected with pmAEQmut (control) or with pmAEQmut/14-3-3ε. However, under these conditions, the influx of massive amounts of Ca^{2+} into the subplasmalemmal region discharged the aequorin probe, and the values of $[Ca^{2+}]_{pm}$ obtained were largely artifactual, as reported previously (16). To avoid saturation of the aequorin probe in subsequent experiments, cells were thus challenged with a lower extracellular $[Ca^{2+}]$. At 100 μM (data not shown) and 20 μM (Fig. 4*A*) extracellular $[Ca^{2+}]$, $[Ca^{2+}]_{pm}$ was higher in 14-3-3ε-transfected cells (9.60 ± 1.50 μM) than in control cells (5.97 ± 0.90 μM; $p < 0.01$). This indicated that Ca^{2+} efflux occurred with faster kinetics in control cells, as would be expected from the inhibition of PMCA4 activity by 14-3-3ε.

Comparison of the Inhibitory Effects of 14-3-3ε on the Activities of the PMCA4 and PMCA2 Pumps—As mentioned in the Introduction, one aspect of the PMCA pumps that is not understood is the rationale for the multiplicity of isoforms and for their tissue-specific expression. Isoform-specific interaction with protein partners, which could differentially modulate pump activity, is an attractive possibility. Although the 14-3-3ε protein interacted with PMCA4, but not with PMCA2, we still considered it interesting to study whether 14-3-3ε has an inhibitory effect on PMCA2 as well.

PMCA4 and PMCA2 were thus cotransfected in HeLa cells with 14-3-3ε and cytAEQ. The amplitude and kinetics of the $[Ca^{2+}]_c$ transient evoked by histamine stimulation (Fig. 4*B*) confirmed previous results (4) showing that PMCA2 is more effective in restoring the basal cytosolic Ca^{2+} level than PMCA4 (peak amplitude of 1.92 ± 0.09 μM ($n = 8$) in hPMCA2-overexpressing cells *versus* 2.68 ± 0.06 μM ($n = 8$) in hPMCA4-overexpressing cells; $p < 0.01$). In any case, both PMCA isoforms induced a significant reduction of the cytosolic response observed in control cells (peak value of 2.95 ± 0.12 μM ($n = 15$)). However, at variance with PMCA4, the amplitude and duration of the agonist-dependent $[Ca^{2+}]$ increase in PMCA2-overexpressing cells were not significantly affected by overexpression of the 14-3-3ε protein (peak amplitude of 1.90 ± 0.05 μM ($n = 16$) in hPMCA2/14-3-3ε-overexpressing cells). The extrusion rates at a fixed $[Ca^{2+}]_c$ of 1.5 μM were 0.193 ± 0.015 μM/s ($n = 8$) in hPMCA2-overexpressing cells *versus* 0.191 ± 0.010 μM/s ($n = 16$) in hPMCA2/14-3-3ε-overexpressing cells. In contrast, 14-3-3ε overexpression inhibited the Ca^{2+}-exporting activity of PMCA4 (peak amplitude of 3.13 ± 0.07 μM ($n = 12$) in hPMCA4/14-3-3ε-overexpressing cells *versus* 2.68 ± 0.06 μM ($n = 8$) in hPMCA4-overexpressing cells; $p < 0.01$), and the height of the cytosolic calcium response was increased by ~13% with respect to control cells and by ~28% with respect to PMCA4-overexpressing cells (Fig. 4*B*). The extrusion rates at a fixed $[Ca^{2+}]_c$ of 2 μM were 0.132 ± 0.010 μM/s ($n = 12$) in hPMCA4/14-3-3ε-overexpressing cells *versus* 0.158 ± 0.011 μM/s ($n = 8$) in hPMCA4-overexpressing cells ($p < 0.01$). These data further confirmed the inhibitory effect of 14-3-3ε on PMCA4 activity.

DISCUSSION

Plasma membrane Ca^{2+} pumps, which have been traditionally less popular as a research topic than the SERCA pump, are now attracting increasing attention. One reason for the expanding interest may be recent evidence suggesting that these pumps could have additional functions in cell signaling besides the long recognized role in clearing cells of Ca^{2+} (10). However, another reason is the increasing number of studies showing that the unusually large number of PMCA isoforms, far from being a biochemical oddity, is likely to reflect the differential Ca^{2+} homeostasis demands of cells in various tissues. The suggestion would be strongly substantiated if the various pump isoforms, including their splicing products, had inherently different functional properties. Evidence that this may be so is now beginning to accumulate, but most results have been gathered using pump preparations separated from the native cellular environment. Thus, some of the differences that have been documented, *e.g.* those on the effect of calmodulin, tend to disappear when the pump variants are studied *in vivo* (4). An alternative way to rationalize the multiplicity of isoforms and to place it in the context of cellular Ca^{2+} regulation would be by postulating isoform-specific pump interactors, which could differentially influence the function of the pumps and/or their distribution along the plasma membrane contour. The matter of partners of the PMCA pump is now becoming a topic of interest. A number of recent studies have identified interacting proteins, with the first reports showing that the C-terminal domain of the pump binds the membrane-associated guanylate kinase via the PDZ domain (7, 8), whereas other studies have shown the pump interacts with Na^+/H^+ exchanger regulatory factor-2 (6), the calcium/calmodulin-dependent serine protein kinase (9), and the neuronal form of NO synthase (10). Other studies have shown interactions with the pro-apoptotic tumor suppressor Ras-associated factor-1 via a domain in the large cytosolic loop that contains the active site (17) and with the catalytic domain of the calcineurin A subunit (18). However, only the study on regulatory factor-2 of the Na^+/H^+ exchanger has suggested the possibility that protein partners interact only with some isoforms of the pump. If such an isoform-specific interaction occurs and has effects on the activity of the pump, it would conveniently rationalize the multiplicity of its isoforms. The work presented here has indeed shown that one protein (14-3-3ε) interacted with PMCA4, but not with PMCA2, and has shown that the interaction had a clear inhibitory effect on the activity of PMCA4, which was not shared by PMCA2. Notably, we have demonstrated the inhibitory effect by studying the pump in the native intracellular environment. Although isoforms 4 and 2 were initially chosen as representative of the ubiquitous and tissue-specific pump variants, respectively, the study will now have to be extended to the other ubiquitous (PMCA1) and tissue-specific (PMCA3) isoforms. Future work will also consider the stoichiometry and affinity of the interaction between 14-3-3ε and PMCA4.

The finding that the 14-3-3 protein (amino acids 5–55) interacted with PMCA4 was somewhat unexpected, as 14-3-3 proteins are generally considered interactors for phosphothreonine and phosphoserine sites in proteins (19). The PMCA pumps are phosphorylated by protein kinases A and C, but the serine and threonine in the consensus sites are located downstream of the calmodulin-binding domain (protein kinase A) (20) and within the calmodulin-binding domain itself (protein kinase C) (21). Because no protein kinase A and protein kinase C consensus sites are present in the N-terminal region of the pump that was used as bait, it must be assumed that, in the case of PMCA4, the 14-3-3ε protein interacted with a non-phosphorylated sequence. This has already been shown to occur in a very small proportion of the total number of 14-3-3 partners (22–24).

The 14-3-3 family of proteins, which are small acidic proteins found only

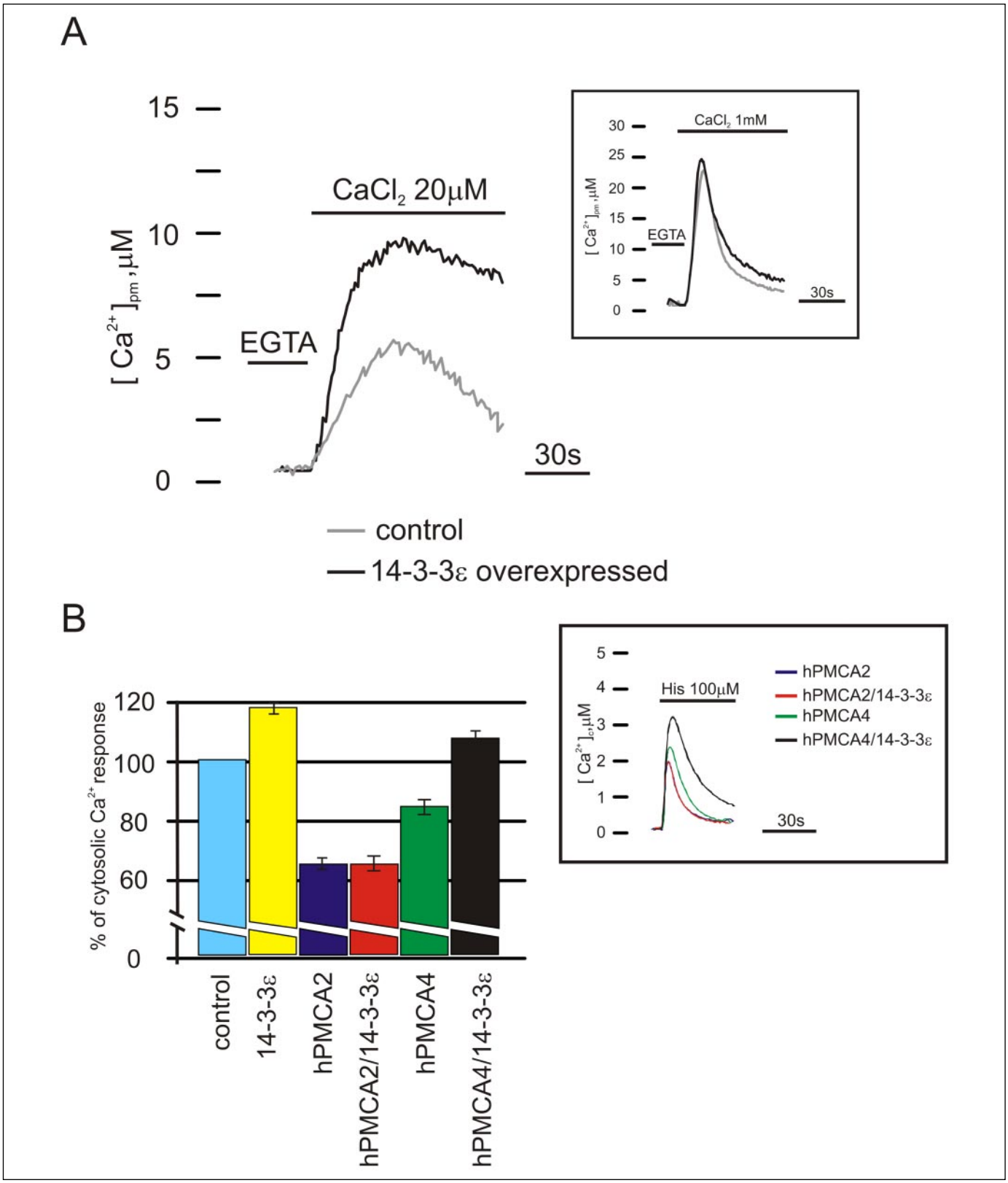

FIGURE 4. **Inhibitory effect of 14-3-3ε on the extruding ability of PMCA4.** *A*, effect of Ca^{2+} re-addition (20 μM and 1 mM $CaCl_2$ (*inset*)) to cells cotransfected with pmAEQmut and 14-3-3ε (*14-3-3ε overexpressed*, *black trace*) or transfected with pmAEQmut (*control*, *gray trace*). This probe allowed the estimation of $[Ca^{2+}]_{pm}$ under conditions of active Ca^{2+} influx through plasma membrane channels. Under these conditions at 1 mM $CaCl_2$, the large increase in $[Ca^{2+}]$ in the subplasmalemmal region saturated the probe (*inset*). Conversely, at 20 μM $CaCl_2$, $[Ca^{2+}]_{pm}$ was markedly higher in 14-3-3ε-transfected cells than in control cells, whereas the kinetics of Ca^{2+} efflux across the plasma membrane was markedly slower. *B*, effect of 14-3-3ε overexpression on the activities of PMCA2 and PMCA4. HeLa cells were transfected with hPMCA4 or hPMCA2 or cotransfected with 14-3-3ε. *Inset*, the $[Ca^{2+}]_c$ measurements were performed with cytAEQ, and the cells were challenged with histamine (*His*) where indicated. The $[Ca^{2+}]_c$ peaks evoked by the agonist under the different experimental conditions are expressed as a percent of the $[Ca^{2+}]_c$ peak in non-transfected cells. Representative traces are shown in the *inset*.

in eukaryotes, influences a very large number of cellular processes. These proteins may complement the effects of phosphorylation by inducing conformational changes in the interacting proteins and/or by affecting their interactions with other partners (25). They may also influence the subcellular distribution of (phosphorylated) interactors. The number of proteins that interact with 14-3-3 proteins has been recently estimated to exceed 200 based on a scaled-up affinity purification technique (26). These 200 proteins influence a large spectrum of functions, from primary metabolism to gene transcription, protein trafficking, and signaling processes. Several of the 14-3-3 interactors are even involved in important diseases, *e.g.* cancer, diabetes, and Parkinson disease.

Although it is tacitly assumed that the functions of 14-3-3 proteins are somehow related to phosphorylated proteins, a role must nevertheless also exist for the (minority of) documented cases in which the interaction does not involve phosphorylated residues. The finding in this study that Ca^{2+} signaling appears to be the target of 14-3-3 via the inhibition of an important non-phosphorylated enzyme thus acquires special significance. However, it also creates a problem: the reversibility of the inhibitory interaction. If the interaction with 14-3-3 is to have regulatory function on the activity of the pump *in vivo*, as one would like to think, ways must necessarily exist to reverse the inhibitory interaction. This would be easy to achieve if 14-3-3 would interact with a phosphorylated residue in the pump, but is much harder to imagine for an interaction not involving phosphoserines or phosphothreonines. In principle, reversibility could be influenced by changes in the concentration of 14-3-3ϵ locally available to the PMCA pump, *i.e.* by fluctuations in the subplasmalemmal domain. Albeit highly unlikely, the occurrence of such changes cannot be ruled out. At the moment, the mechanism(s) to induce reversibility must remain an open question.

Of the 14-3-3 isoforms tested, only the ϵ-isoform interacted with the PMCA pump. The number of 14-3-3 isoforms in various organisms ranges from two in yeast to 12 in *Arabidopsis*. Although recent information suggests that the isoforms may be differentially regulated spatially and temporally, very little is known about the isoform-specific functions. The recent finding that specifically relates deletions in the gene coding for 14-3-3ϵ (which interacts with the PMCA pump) to a severe grade of genetic lissencephaly with complete agyria, the Miller-Dieker syndrome (27), is thus of particular interest.

Acknowledgments—We thank G. Szabadkai (University of Ferrara) for help with two-hybrid system assays and V. Guaran (University of Ferrara) for technical assistance.

REFERENCES

1. Hilfiker, H., Guerini, D., and Carafoli, E. (1994) *J. Biol. Chem.* **269,** 26178–26183
2. Elwess, N. L., Filoteo, A. G., Enyedi, A., and Penniston J. T. (1997) *J. Biol. Chem.* **272,** 17981–17986
3. Guerini, D., Pan, B., and Carafoli, E. (2003) *J. Biol. Chem.* **278,** 38141–38148
4. Brini, M., Coletto, L., Pierobon, N., Kraev, N., Guerini, D., and Carafoli, E. (2003) *J. Biol. Chem.* **278,** 24500–24508
5. Chicka, M. C., and Strehler, E. E. (2003) *J. Biol. Chem.* **278,** 18464–18470
6. DeMarco, S. J., Chicka, M. C., and Strehler, E. E. (2002) *J. Biol. Chem.* **277,** 10506–10511
7. DeMarco, S. J., and Strehler, E. E. (2001) *J. Biol. Chem.* **276,** 21594–21600
8. Kim, E., DeMarco, S. J., Marfatia, S. M., Chishti, A. H., Sheng, M., and Strehler, E. E. (1998) *J. Biol. Chem.* **273,** 1591–1595
9. Schuh, K., Uldrijan, S., Gambaryan, S., Roethlein, N., and Neyses, L. (2003) *J. Biol. Chem.* **278,** 9778–9783
10. Schuh, K., Uldrijan, S., Telkamp, M., Rothlein, N., and Neyses, L. (2001) *J. Cell Biol.* **155,** 201–205
11. Rizzuto, R., Brini, M., Pizzo, P., Murgia, M., and Pozzan, T. (1995) *Curr. Biol.* **5,** 635–642
12. Carrington, W. A., Lynch, R. M., Moore, E. D., Isenberg, G., Fogarty, K. E., and Fay, F. S. (1995) *Science* **268,** 1483–1487
13. Chiesa, A., Rapizzi, E., Tosello, V., Pinton, P., de Virgilio, M., Fogarty, K.E., and Rizzuto, R. (2001) *Biochem. J.* **335,** 1–12
14. Brini, M., Marsault, R., Bastianutto, C., Alvarez, J., Pozzan, T., and Rizzuto, R. (1995) *J. Biol. Chem.* **270,** 9896–9903
15. Strehler, E. E., and Zacharias, D. A. (2001) *Physiol. Rev.* **81,** 21–50
16. Marsault, R., Murgia, M., Pozzan, T., and Rizzuto, R. (1997) *EMBO J.* **16,** 1575–1581
17. Armesilla, A. L., Williams, J. C., Buch, M. H., Pickard, A., Emerson, M., Cartwright, E. J., Oceandy, D., Vos, M. D., Gillies, S., Clark, G. J., and Neyses, L. (2004) *J. Biol. Chem.* **279,** 31318–31328
18. Buch, M. H., Pickard, A., Rodriguez, A., Gillies, S., Maass, A. H., Emerson, M., Cartwright, E. J., Williams, J. C., Oceandy, D., Redondo, J. M., Neyses, L., and Armesilla, A. L. (2005) *J. Biol. Chem.* **280,** 29479–29487
19. Muslin, A. J., Tanner, J. W., Allen, P. M., and Shaw, A. S. (1996) *Cell* **84,** 889–897
20. James, P. H., Pruschy, M., Vorherr, T. E., Penniston, J. T., and Carafoli, E. (1989) *Biochemistry* **28,** 4253–4258
21. Wang, K. K., Wright, L. C., Machan, C. L., Allen, B. G., Conigrave, A. D., and Roufogalis, B. D. (1991) *J. Biol. Chem.* **266,** 9078–9085
22. Wang, B., Yang, H., Liu Y. C., Jelinek, T., Zhang, L., Ruoslahti, E., and Fu, H. (1999) *Biochemistry* **38,** 12499–12504
23. Masters, S. C., Pederson, K. J., Zhang, L., Barbieri, J. T., and Fu, H. (1999) *Biochemistry* **38,** 5216–5221
24. Petosa, C., Masters, S. C., Bankston, L. A., Pohl, J., Wang, B., Fu, H., and Liddington, R. C. (1998) *J. Biol. Chem.* **273,** 16305–16310
25. MacKintosh, C. (2004) *Biochem. J.* **381,** 329–342
26. Pozuelo Rubio, M., Geraghty, K. M., Wong, B. H., Wood, N. T., Campbell, D. G., Morrice, N., and MacKintosh, C. (2004) *Biochem. J.* **379,** 395–408B. H. C.
27. Cardoso, C., Leventer, R. J., Ward, H. L., Toyo-Oka, K., Chung, J., Gross, A., Martin, C. L., Allanson, J., Pilz, D. T., Olney, A. H., Mutchinick, O. M., Hirotsune, S., Wynshaw-Boris, A., Dobyns, W. B., and Ledbetter, D. H. (2003) *Am. J. Hum. Genet.* **72,** 918–930